Organic & Biomolecular Chemistry

Accepted Manuscript

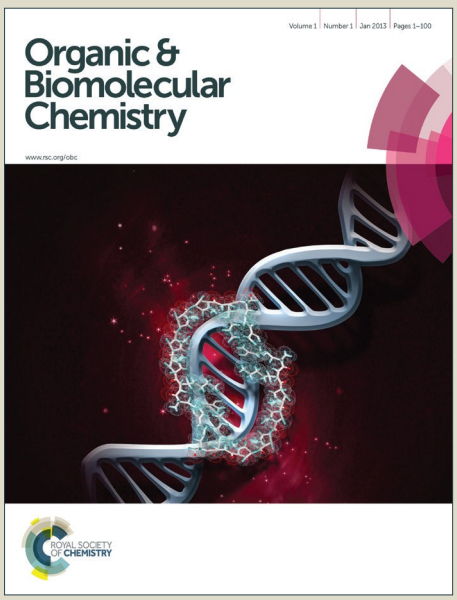

ROYAL SOCIETY OF CHEMISTRY

www.rsc.org/obc

Journal Name

ARTICLE

Maltotriose-Conjugation to Fluorinated Chlorin Derivative Generating PDT Photosensitizer with Improved Water-Solubility

Received 00th January 20xx,
Accepted 00th January 20xx

DOI: 10.1039/x0xx00000x

www.rsc.org/

Atsushi Narumi,*[a] Takahiro Tsuji,[a] Kosuke Shinohara,[a] Hiromi Yamazaki,[b] Moriya Kikuchi,[b] Seigou Kawaguchi,[a] Timoya Mae,[c] Atsushi Ikeda,[c] Yuichi Sakai,[d] Hiromi Kataoka,[e] Masahiro Inoue,[f] Akihiro Nomoto,[g] Jun-ichi Kikuchi,[h] Shigenobu Yano*[h]

Photoactive molecules with the frameworks of chlorin and/or porphyrin possessing four perfluorinated aromatic rings were conjugated with maltotriose (Mal_3) *via* the nucleophilic aromatic substitution reaction and subsequent deprotection reaction of the oligosaccharide moieties. The resulting oligosaccharide-conjugated molecules are ultimately improved as compared to the previously reported monosaccharide-counterparts in terms of water-solubility. In particular, the water-soluble chlorin derivative surrounded by four Mal_3 molecules showed an excellent biocompatibility, strong photoabsorption in the longer wavelength regions, and a very high photocytotoxicity. Thus, the present synthetic route combined with the use of an oligosaccharide was shown to be a straightforward strategy to develop the third generation photosensitizer for photodynamic therapy (PDT).

Introduction

Photodynamic therapy (PDT) is a next-generation minimally invasive tumor treatment by reactive oxygen species (ROS) generated by the photochemical reactions between a photosensitizer and tissue oxygen.[1, 2] Dihydroporphyrin, called chlorin, is a promising photoactive heterocycle framework meeting the requirements of the PDT photosensitizers due to the high ROS generation efficiency and also the strong photoabsorption of longer wavelength light that penetrates deeper into tissues.[1-3] As representative studies, chlorin-type PDT photosensitizers, such as *meso*-tetra(hydroxyphenyl)chlorin,[4] mono-l-aspartyl chlorin e6 (NPe6),[5] and pyropheophorbide derivatives[6] have been reported. In particular, much attention has been directed to the glycoconjugation of chlorin derivatives mainly for the purpose of improving their biocompatibility and tumor-selectivity.[3, 7-18] For example, the chlorin derivative possessing four perfluorinated aromatic rings, such as 5,10,15,20-tetrakis(pentafluorophenyl)-2,3-[methano(*N*-methyl)iminomethano]chlorin (TFPC), was encircled with four glucose (Glc) molecules.[12] The product called G-chlorin (or TFPC-SGlc) (Chart 1) showed a very high photocytotoxicity[14, 15] with the half maximal (50%) inhibitory concentration (IC_{50}) value of 0.5 μM.[12] This result should be mainly related to the fact that the Glc is likely to concentrate on the malignant tumor cells, called the Warburg effect.[19] However, G-chlorin is a molecule insoluble in water, which would be not suitable for intravenous injection. Furthermore, a good water solubility will promise rapid clearance from the body to avoid cutaneous phototoxicity.

In this study, we developed a straightforward strategy to introduce both tumor-selectivity and water-solubility into the chlorin derivatives by using a Glc-derived oligosaccharide, such as maltotriose (Mal_3), with the desire to obtain the next generation water-soluble unimolecular PDT photosensitizer. The synthesis of the target compound, i.e., 5,10,15,20-tetrakis[4-(β-D-maltotriosylthio)-2,3,5,6-tetrafluorophenyl]-2,3-[methano(*N*-methyl)iminomethano]chlorin, called Mal_3-chlorin (or TFPC-SMal_3) (Chart 1), is described together with its characterizations in terms of its photoabsorption properties in water and/or physiological conditions, hydrophilic-hydrophobic parameter, ROS generation efficiency, dark toxicity, and photocytotoxicity. We report the advantage of using oligosaccharides by the comparisons of the properties of Mal_3-chlorin to those of G-chlorin. Similarly, 5,10,15,20-tetrakis(perfluorophenyl)porphyrin (TFPP) was conjugated with Mal_3 and Glc to prepare the porphyrin-counterparts, such as

[a] *Department of Polymer Science and Engineering, Graduate School of Science and Engineering, Yamagata University, Jonan 4-3-16, Yonezawa 992-8510, Japan. E-mail: narumi@yz.yamagata-u.ac.jp*
[b] *Department of Polymer Science and Engineering, Faculty of Engineering, Yamagata University, Jonan 4-3-16, Yonezawa 992-8510, Japan.*
[c] *Department of Applied Chemistry, Graduate School of Engineering, Hiroshima University, 1-4-1, Kagamiyama, Higashi-Hiroshima 739-8527, Japan.*
[d] *R&D Strategy & Market Connection, R&D Planning and Business Development, Asahi Kasei Chemicals Corporation, 1-105 Kanda Jinbocho, Chiyoda-ku, Tokyo 101-8101, Japan.*
[e] *Department of Gastroenterology and Metabolism, Nagoya City University Graduate School of Medical Sciences, Kawasumi, Mizuho-cho, Mizuho-ku, Nagoya 467-8601, Japan.*
[f] *Osaka Medical Center for Cancer and Cardiovascular Diseases, 1-3-3, Nakamichi, Higashinari-ku, Osaka 537-0025, Japan.*
[g] *Department of Applied Chemistry, Graduate School of Engineering, Osaka Prefecture University, 1-1 Gakuen-cho, Naka-ku, Sakai, Osaka 599-8531, Japan.*
[h] *Graduate School of Materials Science, Nara Institute of Science and Technology, Takayama, Ikoma, Nara 630-0192, Japan. E-mail: yano-shigenobu@ms.naist.jp*

†Electronic Supplementary Information (ESI) available: Experimental Section, Spectral data, UV-vis Absorption Property, Quantum Yield of $^1O_2$ generation, Fluorescence Microscopy Measurement, Effect of scavengers. See DOI: 10.1039/x0xx00000x

Mal_3-porphyrin (or TFPP-SMal_3) and G-porphyrin (or TFPP-SGlc), respectively, (Chart 1) and their properties were compared in this study.

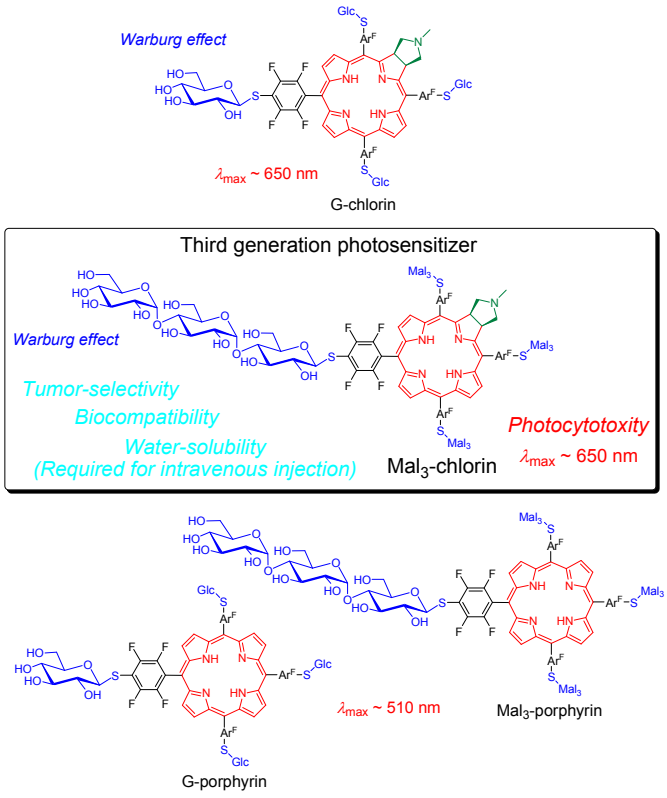

Chart 1. Structures of Mal_3-conjugated photoactive molecules (Mal_3-chlorin and Mal_3-porphyrin) in this study and previously reported Glc-conjugated photoactive molecules (G-chlorin and G-porphyrin).

Results and discussion

Scheme 1 shows a synthetic route for the Mal_3-chlorin as a typical method for the preparation of the four glycoconjugated photosensitizers. 1-Thioacetyl-2,3,6-tri-*O*-acetyl-4-*O*-(2,3,6-tri-*O*-acetyl-4-*O*-(2,3,4,6-tetra-*O*-acetyl-*α*-*O*-glucopyranosyl)-*α*-D-glucopyranosyl)-*β*-D-glucopyranose[20, 21] ($AcMal_3$-SAc) was prepared according to the literature and combined with TFPC[22] using diethylamine (Et_2NH) as a base. The reactivity of this nucleophilic aromatic substitution reaction was significantly high as compared to that of the 5,10,15,20-tetrakis(perfluorophenyl)porphyrin (TFPP) with $AcMal_3$-SAc (see Supplementary Information). The optimal condition is that a 4.2 equivalent amount of $AcMal_3$-SAc was slowly added to the TFPC solution in dry DMF in the presence of Et_2NH with cooling at 0 °C. After the addition, the mixture was stirred for 4 hours at room temperature. As judged by the TLC analysis, the reaction produced the target 5,10,15,20-tetrakis[4-(deca-*O*-acetyl-*β*-D-maltotriosylthio)-2,3,5,6-tetrafluorophenyl]-2,3-[methano(*N*-methyl)iminomethano]chlorin called $AcMal_3$-chlorin (or TFPC-S$AcMal_3$) as the main product together with a small amount of the tris-substituted chlorin derivatives as byproducts. The main product could be isolated as a blackish-green solid by silica gel column chromatography. In the ^1H NMR spectrum of the product, the characteristic signals due to the *β*-pyrrole protons and inner amine protons appeared at 8.9-8.4 ppm and -1.8 ppm, respectively, together with those due to methylene protons in the pyrrolidine ring at 3.1 and 2.5 ppm (Fig. S1). The signals due to the $AcMal_3$ unit were observed in the regions of 5.5-3.9 and 2.2-2.0 ppm. For the ^{19}F NMR spectrum of the product, the signal due to the fluorines at the *meta*- and *ortho*-positions in the aromatic rings appeared in the region between -130 and -137 ppm (Fig. S1), indicating that the substitution reaction selectively occurred at the *para*-positions. The ESI-MS exhibited the main peak at m/z = 4713.10, which fairly agreed with the calculated $[M+H]^+$ value for the target compound of 4713.04. These results indicated that the product was assigned to the target precursor $AcMal_3$-chlorin (Scheme 1). It should be noted that the coupling constant between the *S*-linked anomeric H-1 proton and H-2 proton was 10.0 Hz as determined by the ^1H NMR analysis. This value was in good agreement with the coupling constant between the H-1 and H-2 protons in the axial positions for the chair-form glucopyranose (generally between 8 Hz and 10 Hz). Hence, we confirmed that the main product, $AcMal_3$-chlorin, was assigned to the tetrakis-*β*-*S*-glycosylated derivatives. In this study, $AcMal_3$-porphyrin (or TFPP-S$AcMal_3$) was also newly prepared *via* a similar method (Fig. S2).

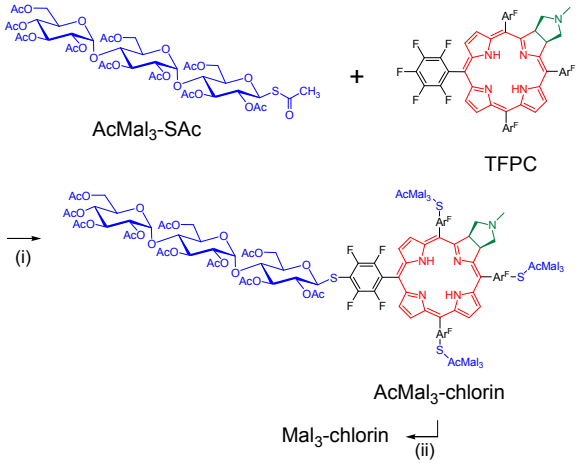

Scheme 1. Synthesis of Mal_3-chlorin by (i) nucleophilic aromatic substitution reaction using Et_2NH (ii) and deacetylation using sodium methoxide (NaOMe).

The deacetylation of $AcMal_3$-chlorin was performed by the treatment with sodium methoxide (NaOMe) in dry THF to afford Mal_3-chlorin as a green solid. The accomplishment of the deacetylation was confirmed by the FT-IR spectra (Fig. S3 and Fig. S4). The purity of Mal_3-chlorin determined by the LC-MS measurement was 96.9 %. The LC-MS measurement also indicated that the degree of the deacetylation was 98.6 %. Similarly, Mal_3-porphyrin (Chart 1) was obtained as brownish-red solid. A crucial superiority of the Mal_3-series to the G-series was observed regarding their water-solubility. Mal_3-chlorin and Mal_3-porphyrin were readily solubilized in water, producing green and brown aqueous solutions, respectively. The water-solubility of Mal_3-chlorin was > 37 mg/mL. In order to quantify the introduced hydrophilicity, we determined the partition coefficient (log *P*) that is defined by the following equation.

$$\log P = \log \frac{[C_{octanol}]}{[C_{PBS}]}$$

where $[C_{octanol}]$ and $[C_{PBS}]$ denote the concentrations of the glycoconjugated photosensitizers being portioned into the 1-octanol phase and the PBS buffer phase, respectively. The log *P* values were -1.78 for Mal$_3$-chlorin, -1.67 for Mal$_3$-porphyrin, 0.13 for G-chlorin, and 0.58 for G-porphyrin. This means that the water-solubility of Mal$_3$-chlorin is 45 times higher than that of G-chlorin. It should be noted that the log *P* values of the Mal$_3$-series were similar to that of -1.58 for talaporfin (NPe6[5]) that is currently in clinical use.

The UV-vis absorption property for Mal$_3$-chlorin and Mal$_3$-porphyrin together with those of TFPC and TFPP were examined and summarized in Table S1. We now discuss the absorptions due to the Q band at the wavelengths around 650 nm, the longer wavelengths regions favorable for the permeability of physiological tissues. The left panel in Fig. 1 displays the UV-vis spectra of Mal$_3$-chlorin and TFPC. In DMSO, Mal$_3$-chlorin showed an absorption at the maximum absorption wavelength (λ_{max}) of 652 nm with the molar absorption coefficient (ε) of 33400 M^{-1} cm^{-1} (green solid line). This was similar to that of TFPC with the λ_{max} (ε) value of 652 nm (41600 M^{-1} cm^{-1}) in DMSO (green dashed line). A more crucial result in this study is the photochemical properties in the aqueous media (black lines in both the left and right panels). The UV-vis profile in water (left panel) was very similar to that in PBS (right panel). The λ_{max} (ε) values were 649 nm (34600 M^{-1} cm^{-1}) in water and 651 nm (35900 M^{-1} cm^{-1}) in PBS buffer. The result to be further emphasized is that the profile of Mal$_3$-chlorin in the aqueous media was very similar to that in DMSO. Consequently, Mal$_3$-chlorin showed the featured photochemical properties derived from the TFPC framework even under physiological conditions. Similarly, Mal$_3$-porphyrin showed the adsorptions in water originated from the TFPP unit (Fig. S5).

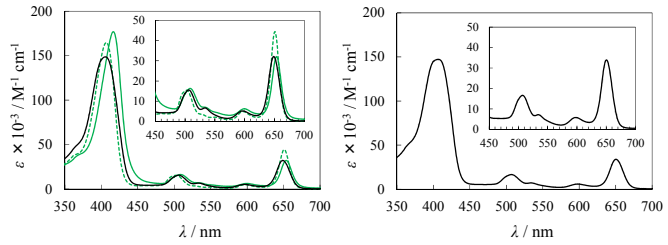

Fig. 1. UV-vis spectra of Mal$_3$-chlorin in DMSO (green solid line), TPFC in DMSO (green dashed line), and Mal$_3$-chlorin in water (black solid line) (left panel) and Mal$_3$-chlorin in PBS buffer (right panel).

The singlet oxygen ($^1O_2$) generation by the glycoconjugated photosensitizers was determined by the photobleaching of 9,10-anthracenediyl-bis(methyl)dimalonic acid (ABDA) at 400 nm (λ_{max} of ABDA).[23] Figure 2 shows the plot of the degradation of ABDA as a function of the photoexposure time, indicating that the amount of $^1O_2$ generated by the chlorin-series was much higher than that by the porphyrin-series. The Abs/Abs$_0$ value gave similar curves for the Mal$_3$-chlorin and G-chlorin in aqueous media. Thus, Mal$_3$-chlorin was shown to be the compound generating $^1O_2$ by photoirradiation in a very high efficiency comparable to that of G-chlorin. It should be noted that Mal$_3$-chlorin produced $^1O_2$ in the oxygen-saturated D_2O solutions by photoirradiation (532 nm), which could be quantified from the peak area due to the $^1O_2$ phosphorescence at 1270 nm (Fig. S8). The quantum yield of $^1O_2$ generation from Mal$_3$-chlorin was determined to be 0.28, which is much larger than that from NPe6 (0.08) (Table S2).

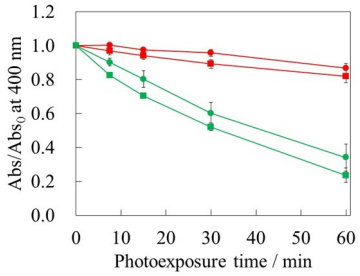

Fig. 2. Time-dependent bleaching of ABDA caused by the $^1O_2$ generated from Mal$_3$-chlorin (green circle), Mal$_3$-porphyrin (red circle), G-chlorin (green square), and Mal$_3$-porphyrin (red square). Changes in the ABDA absorption at 400 nm upon photoirradiation (> 600 nm, 15 mW cm^{-2}) were monitored as a function of time (Abs$_0$: initial absorbance). [Sample] = 15 μM, [ABDA] = 2.5 mM: under an oxygen atmosphere at 25 °C.

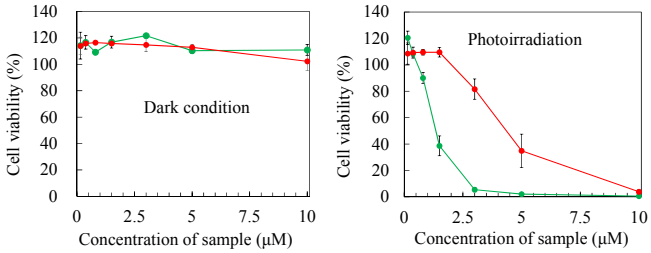

Fig. 3. Plot of cell-viability vs. concentration of Mal$_3$-chlorin (green circle) and Mal$_3$-porphyrin (red circle) for the photo-unirradiated system (left panel) and irradiated system (610–740 nm, 30 min) (right panel). Each value represents the mean ±SD of three experiments.

The photodynamic activities of Mal$_3$-chlorin and Mal$_3$-porphyrin were evaluated using human cervical cancer Hela cells. The sample was added to the cell medium and its final concentrations were adjusted to 0.15, 0.34, 0.75, 1.5, 3.0, 5.0, and 10.0 μM. Using the WST-8 assay, the cell viability was measured in light-unirradiated and irradiated cells as a ratio (%) compared to untreated cells. It should be noted that these PDT tests did not contain any organic solvents due to the high water-solubility of the Mal$_3$-series. Fig. 3 is a plot of the cell-viability as a function of the concentrations of the Mal$_3$-series photosensitizers. For the light-unirradiated systems, no cell was killed by both the Mal$_3$-chlorin and Mal$_3$-porphyrin systems at concentrations ranging from 0.15 to 10.0 μM. Thus, the Mal$_3$ unit was shown to be a powerful tool to introduce biocompatibility. On the other hand, under the irradiation of light at wavelength above 610 nm, the cell viability reduced to 35 % for the Mal$_3$-porphyrin system when its concentration was 5.0 μM. A very high photodynamic activity was observed for the Mal$_3$-chlorin system in which almost all cells (95 %) were killed when the concentration was the very low value of 3.0 μM. The half maximal (50%) inhibitory concentration (IC$_{50}$) value of

Mal_3-chlorin was determined to be approximately 1.3 μM for the present assay system. Fig. S6 displays the phase contrast and fluorescence images of the HeLa cells after being treated with the glycoconjugated photosensitizers (4.0 μM) for 24 h at 37 ºC, suggesting that both Mal_3-chlorin and Mal_3-porphyrin were incorporated into the cells. This result also implied that there was no remarkable differences between the two glycoconjugated photosensitizers regarding the cellular uptake efficiency. The effect of D-mannitol and L-histidine, the scavengers of hydroxyl radicals and $^1O_2$, respectively,[24,25] on the Mal_3-chlorin system was examined according to the method reported elsewhere.[26] The photodynamic activities of Mal_3-chlorin were blocked by L-histidine, whereas D-mannitol was ineffective (Fig. 4). This result supported that the active species for the Mal_3-chlorin system was assignable to $^1O_2$ generated *via* the reaction called an energy transfer type II reaction. Thus, the high photodynamic activity of Mal_3-chlorin would be attributable to the high $^1O_2$ generation efficiency that originated from the TFPC moieties. Consequently, the Mal_3-conjugation of TPFC was shown to produce an *in vivo* injectable advanced photosensitizer with an excellent biocompatibility and high PDT activity especially due to the positive accumulation nature of the Mal_3 unit toward tumor cells.

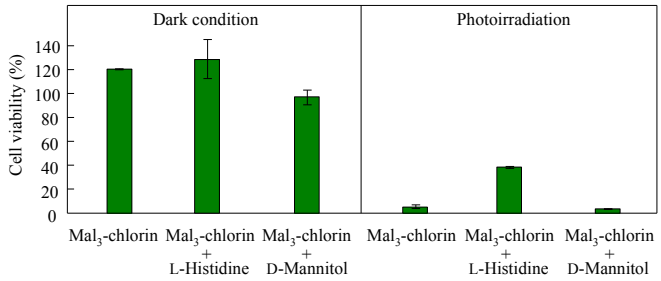

Fig. 4. Effect of ROS scavengers on photodynamic activity of Mal_3-chlorin. Photodynamic activity of Mal_3-chlorin (3 μM) was measured in the presence of 50 mM L-histidine or 50 mM D-mannitol. Each value represents the mean ±SD of three experiments.

Conclusions

Mal_3-chlorin was prepared as a complement to G-chlorin. As for the $^1O_2$ generation efficiency and photocytotoxicity, Mal_3-chlorin was proved to have a very high performance comparable to that of G-chlorin. The crucial advantage of Mal_3-chlorin was water-solubility, which would allow its intravenous injection without the use of toxic organic solvents. The hydrophilic/hydrophobic balance of Mal_3-chlorin was determined to be similar to that of talaporfin, while the IC_{50} value of Mal_3-chlorin was very low (ca. 1.3 μM for the present assay system). Thus, the newly developed water-soluble Mal_3-chlorin is a candidate as the third generation unimolecular photosensitizer for PDT.

Acknowledgements

The authors acknowledge Hayashibara Co., Ltd., Japan, for providing the maltotriose (Mal_3). This study was financially supported by JSPS KAKENHI grant numbers 19350031, 23590923, 25288028, 26460947, the Japan-German Exchange Program supported by the JSPS and the Deutsche Forschungsgemeinschaft (DFG), and by the Japan Advanced Molecular Imaging Program (J-AMP) of the Ministry of Education, Culture, Sports, Science and Technology of Japan, and partially supported by the Translational Research Network Program (Ministry of Education, Culture, Sports, Science, & Technology) from the Japan Agency for Medical Research and Development, AMED and a grant from the San-Ei-Gen Foundation for chemical research.

Experimental

Synthesis of 5,10,15,20-tetrakis[4-(deca-*O*-acetyl-*β*-D-maltotriosylthio)-2,3,5,6-tetrafluorophenyl]-2,3-[methano(*N*-methyl)iminomethano]chlorin ($AcMal_3$-chlorin)

The mixture of TPFC (0.18 g, 0.18 mmol) and Et_2NH (1.2 mL) in dry DMF (60 mL) was stirred at 0 ºC under a nitrogen atmosphere. To the mixture, $AcMal_3$-SAc (0.81 g, 0.83 mmol) in dry DMF (20 mL) was dropwise added. After being stirred for 4 hours at room temperature under a nitrogen atmosphere, the mixture was transferred to a separating funnel, $CHCl_3$ (100 mL) and water (100 mL) were added, and the organic layer was separated. The aqueous layer was extracted with chloroform (50 mL × 3) and the combined organic layers were washed with water and dried over sodium sulfate then evaporated to dryness. The residue was purified by flash column chromatography (silica gel; $CHCl_3$/EtOAc, 1:2) to give $AcMal_3$-chlorin as a blackish green solid (0.28 g, 33 %). R_f = 0.37 ($CHCl_3$/EtOAc, 1:2). ^{1}H-NMR (400 MHz, $CDCl_3$, Si $(CH_3)_4$ = 0 ppm) : δ (ppm) = 8.82-8.85 (2H, m, 8,17-*β*-pyrrole *H*), 8.58 (2H, brs, 12,13-*β*-pyrrole *H*), 8.48-8.49 (2H, m, 7,18-*β*-pyrrole *H*), 5.31-5.42 (20H, m, *H*-$1^{Mal2\text{-}Mal3}$, *H*-$3^{Mal1\text{-}Mal3}$), 5.14 (4H, d, $J_{1,2}$ = 10.0 Hz, *H*-1^{Mal1}), 4.94-5.09 (8H, m, *H*-2^{Mal}, *H*-4^{Mal3}), 4.84-4.87 (4H, m, *H*-2^{Mal2}), 4.74-4.78 (4H, m, *H*-2^{Mal3}), 4.30-4.69 (12H, m, *H*-$6^{Mal1\text{-}Mal3}$), 3.88-4.26 (32H, m, *H*-$4^{Mal1\text{-}Mal2}$, *H*-$5^{Mal1\text{-}Mal3}$, *H*-$6'^{Mal1\text{-}Mal3}$), 2.00-2.18 (120H, s, C*H*$_3$), -1.76 (brs, 2H, N*H*). ^{19}F-NMR (376 MHz, $CDCl_3$) : δ (ppm) = -130.11, -130.36 (1F, m, 3,5-Ph*F*), -130.85 (1F, brs, 3,5-Ph*F*), -131.65 (2F, s, 3,5-Ph*F*), -134.57, -134.78 (1F, m, 2,6-Ph*F*), -136.14 (2F, s, 2,6-Ph*F*), -136.69, -136.87 (1F, m, 2,6-Ph*F*). ^{13}C-NMR (100 MHz, $CDCl_3$ = 77 ppm) : δ (ppm) = 170.69, 170.59, 170.42, 170.20, 169.93, 169.79, 169.53 (-O*C*OCH$_3$), 152.45 (1,4,11,14-*α*-pyrrole *C*), 148.43-144.81 (2,6 Ph-*C*, 3,5 Ph-*C*), 140.11 (9,16-*α*-pyrrole *C*), 135.05 (6,19-*α*-pyrrole *C*), 132.65 (8,17-*β*-pyrrole *C*), 128.53 (12,13-*β*-pyrrole *C*), 124.50, 124.11 (7,18-*β*-pyrrole *C*), 122.26 (4 Ph-*C*), 111.71 (1 Ph-*C*), 106.76 (10,15-*meso* *C*), 97.52 (5,20-*meso* *C*), 95.94, 95.74 (*C*-$1^{Mal2\text{-}Mal3}$), 83.91 (*C*-1^{Mal1}), 76.37, 73.44, 72.46, 71.80, 71.29, 70.55, 70.13, 69.39, 69.16, 68.60, 67.96 (*C*-$2^{Mal1\text{-}Mal3}$, *C*-$3^{Mal1\text{-}Mal3}$, *C*-$4^{Mal1\text{-}Mal3}$, *C*-$5^{Mal1\text{-}Mal3}$), 62.60, 62.32, 61.44 (*C*-$6^{Mal1\text{-}Mal3}$), 53.18 (2,3-*β*-pyrrole *C*), 41.34 (N-*C*H$_3$), 21.0, 20.88, 20.81, 20.75, 20.68 (-OCO*C*H$_3$). FT-IR (KBr): ν (cm^{-1}) = 1753, 1471, 1371, 1234, 1043, 972. ESI-TOF MS (*m*/*z*) calcd for $[M + Na]^+$, 4713.10; found, 4713.06. UV-vis (*c* = 5.00 μM, DMSO, path

length = 1 cm, 25 °C): λ / nm ($\varepsilon \times 10^{-3}$ /M^{-1} cm^{-1}) = 412 (176), 505 (16.4), 537 (4.06), 598 (5.49), 652 (35.9).

Synthesis of 5,10,15,20-Tetrakis[4-(*β*-D-maltotriosylthio)-2,3,5,6-tetrafluorophenyl]-2,3-[methano(*N*-methyl)iminomethano]chlorin (Mal_3-chlorin).

$AcMal_3$-chlorin (37 mg, 7.9 μmol) was dissolved in dry THF (3.5 mL) in a Teflon® bottle containing a magnetic stir bar. To the bottle, 2.0 wt% NaOMe in dry a THF solution (0.9 mL) was slowly added. The mixture was stirred at room temperature for 24 h under a nitrogen atmosphere with blocking the light. After formation of the target product was confirmed by TLC (ODS plate; H_2O/CH_3CN, 1:1; R_f = 0.46), the mixture was neutralized by acetic acid then diluted by MeOH. The residue was dialyzed against water using Spectra/Por® dialysis tubing (MWCO 1,000) for 2 days and then freeze-dried to give Mal_3-chlorin as a green solid (15 mg, 63 %). FT-IR (KBr): ν (cm^{-1}) = 3394, 1470, 1029. LC-MS (*m*/*z*) calcd, 3032.68 $[M + H]^+$ for $C_{119}H_{142}F_{16}N_5O_{60}S_4$; found, 1525.36 $[M + H + NH_4]^{2+}$ + 1017.24 $[M + 2H + NH_4]^{3+}$ (M, 62.3 %), *m*/*z* = 1546.36 $[M + H + NH_4]^{2+}$ + 1031.24 $[M + 2H + NH_4]^{3+}$ (M + 1Ac, 20.0 %), *m*/*z* = 1567.37 $[M + H + NH_4]^{2+}$ + 1045.25 $[M + 2H + NH_4]^{3+}$ (M + 2Ac, 10.7 %), *m*/*z* = 1588.37 $[M + H + NH_4]^{2+}$ + 1059.25 $[M + 2H + NH_4]^{3+}$ (M + 3Ac, 2.1 %), *m*/*z* = 1609.38 $[M + H + NH_4]^{2+}$ + 1078.93 $[M + 2H + NH_4]^{3+}$ (M + 4Ac, 1.6 %). UV-vis (*c* = 5.00 μM, H_2O, path length = 1 cm, 25 °C): λ / nm ($\varepsilon \times 10^{-3}$ /M^{-1} cm^{-1}) = 407 (148), 507 (16.6), 536 (7.17), 597 (5.85), 649 (34.9).

Notes and references

1 S. Yano, S. Hirohara, M. Obata, Y. Hagiya, S. Ogura, A. Ikeda, H. Kataoka, M. Tanaka and T. Joh, *J. Photochem. Photobiol. C: Photochem. Rev.*, 2011, **12**, 46-67.

2 N. V. S. Dinesh, K. Bhupathiraju, W. Rizvi, J. D. Batteas and C. M. Drain, *Org. Biomol. Chem.*, 2016, **14**, 389-408.

3 S. Singh, A. Aggarwal, N. V. S. D. K. Bhupathiraju, G. Arianna, K. Tiwari and C. M. Drain, *Chem. Rev.*, 2015, **115**, 10261-10306.

4 R. Bonnett, R. D. White, U. J. Winfield and M. C. Berenbaum, *Biochem. J.*, 1989, **261**, 277-280.

5 J. D. Spikes and J. C. Bommer, *J. Photochem. Photobiol. B*, 1993, **17**, 135-143.

6 Y. Chen, X. Zheng, M. P. Dobhal, A. Gryshuk, J. Morgan, T. J. Dougherty, A. Oseroff and R. K. Pandey, *J. Med. Chem.*, 2005, **48**, 3692-3695.

7 P. Maillard, C. Hery and M. Momenteau, *Tetrahedron Lett.*, 1997, **38**, 3731-3734.

8 Y. Mikata, Y. Onchi, M. Shibata, T. Kakuchi, H. Ono, S. Ogura, I. Okura and S. Yano, *Bioorg. Med. Chem. Lett.* , 1998, **8**, 3543-3548.

9 G. Zheng, A. Graham, M. Shibata, J. R. Missert, A. R. Oseroff, T. J. Dougherty and R. K. Pandey, *J. Org. Chem.*, 2001, **66**, 8709-8716.

10 A. M. G. Silva, A. C. Tome, M. G. P. M. S. Neves, A. M. S. Silva, J. A. S. Cavaleiro, D. Perrone and A. Dondoni, *Tetrahedron Lett.*, 2002, **43**, 603-605.

11 S. Hirohara, M. Obata, H. Alitomo, K. Sharyo, S. I. Ogata, C. Ohtsuki, S. Yano, T. Ando and M. Tanihara, *Biol. Pharm. Bull.*, 2008, **31**, 2265-2272.

12 S. Hirohara, M. Obata, H. Alitomo, K. Sharyo, T. Ando, M. Tanihara and S. Yano, *J. Photochem. Photobiol. B: Biol.*, 2009, **97**, 22-33.

13 M. Obata, S. Hirohara, R. Tanaka, I. Kinoshita, K. Ohkubo, S. Fukuzumi, M. Tanihara and S. Yano, *J. Med. Chem.*, 2009, **52**, 2747-2753.

14 S. Singh, A. Aggarwal, S. Thompson, J. P. C. Tome, X. C. Zhu, D. Samaroo, M. Vinodu, R. M. Gao and C. M. Drain, *Bioconjugate Chem.*, 2010, **21**, 2136-2146.

15 M. Tanaka, H. Kataoka, M. Mabuchi, S. Sakuma, S. Takahashi, R. Tujii, H. Akashi, H. Ohi, S. Yano, A. Morita and T. Joh, *Anticancer Res.*, 2011, **31**, 763-769.

16 S. Hirohara, Y. Kawasaki, R. Funasako, N. Yasui, M. Totani, H. Aitomo, J. Yuasa, T. Kawai, C. Oka, M. Kawaichi, M. Obata and M. Tanihara, *Bioconjugate Chem.*, 2012, **23**, 1881-1890.

17 S. Sakuma, E. Otake, K. Torii, M. Nakamura, A. Maeda, R. Tujii, H. Akashi, H. Ohi, S. Yano and A. Morita, *J. Porphyrins Phthalocyanines*, 2013, **17**, 331-342.

18 A. Aggarwal, S. Thompson, S. Singh, B. Newton, A. Moore, R. M. Gao, X. B. Gu, S. Mukherjee and C. M. Drain, *Photochem. Photobiol.*, 2014, **90**, 419-430.

19 O. Warburg, *Science*, 1997, **123**, 309-314.

20 D. P. Gamblin, P. Garnier, S. van Kasteren, N. J. Oldham, A. J. Fairbanks and B. G. Davis, *Angew. Chem. Int. Ed.*, 2004, **43**, 828-833.

21 H. Oka, T. Koyama, K. Hatano and K. Matsuoka, *Bioorg. Med. Chem.*, 2012, **20**, 435-445.…

22 A. M. G. Silva, A. C. Tome, M. G. P. M. S. Neves, A. M. S. Silva and J. A. S. Cavaleiro, *J. Org. Chem.*, 2005, **70**, 2306-2314.

23 B. A. Lindig, M. A. J. Rodgers and A. P. Schaap, *J. Am. Chem. Soc.*, 1980, **102**, 5590-5593.

24 S. Goldstein, G. Czapski, *Int. J. Radiol.*, 1984, **46**, 725–729.

25 B. A. Lindig, M. A. J. Rodgers, *Photochem. Photobiol.,* 1981, **33**, 627–634.

26 A. Ikeda, M. Akiyama, T. Ogura, T. Takeya, *ACS Med. Chem. Lett.,* 2010, **1**, 115–119.